Quark polarization in a viscous quark-gluon plasma

Xu-Guang Huang,[1,2] Pasi Huovinen,[2] and Xin-Nian Wang[3,4,2]
[1]*Frankfurt Institute for Advanced Studies, D-60438 Frankfurt am Main, Germany*
[2]*Institut für Theoretische Physik, Goethe-Universität, D-60438 Frankfurt am Main, Germany*
[3]*Institute of Particle Physics, Central China Normal University, Wuhan, 430079, China*
[4]*Nuclear Science Division, MS 70R0319, Lawrence Berkeley National Laboratory, Berkeley, California 94720, USA*
(Received 21 September 2011; published 21 November 2011)

Quarks produced in the early stage of noncentral heavy-ion collisions could develop a global spin polarization along the opposite direction of the reaction plane due to the spin-orbital coupling via parton interaction in a medium that has finite longitudinal flow shear along the direction of the impact parameter. We study how such polarization evolves via multiple scattering in a viscous quark-gluon plasma with an initial laminar flow. The final polarization is found to be sensitive to the viscosity and the initial shear of local longitudinal flow.

DOI: 10.1103/PhysRevC.84.054910 PACS number(s): 13.88.+e, 12.38.Mh, 25.75.Nq

I. INTRODUCTION

The observed jet quenching and collective phenomena in high-energy heavy-ion collisions at the Relativistic Heavy Ion Collider (RHIC) provide strong evidence of the formation of strongly coupled quark-gluon plasma (QGP) [1,2]: The strong quenching of high transverse momentum jets is understood to be caused by parton energy loss induced by multiple collisions of the leading parton with color charges in the thermal medium [3–8]; the observed collective flow in the final bulk hadron spectra indicates a hydrodynamic behavior of the initial dense matter as an almost perfect fluid with a very small shear viscosity [9,10], $\eta/s \lesssim 0.5$. The large jet transport parameter from the observed strong jet quenching and small shear viscosity inferred from the collective flow can be connected to each other through a transport process in a strongly coupled system [11]. They both describe the ability of the medium partons to transfer momentum via strong interaction in QCD and maintain local equilibrium. Globally, such transport processes help to dissipate variations of flow velocities and thus will reduce the anisotropic flow, which is driven by the initial geometric anisotropy [9,10]. In this paper, we discuss the possibility of global quark spin polarization caused by such transport processes in noncentral high-energy heavy-ion collisions.

It was first proposed by Liang and Wang [12] that global quark polarization could occur in the QGP formed in a noncentral heavy-ion collision. They argued that at a finite impact parameter, the initial partons produced in the collision can develop a longitudinal fluid shear distribution representing local relative orbital angular momentum (OAM) in the same direction as the global OAM of the noncentral nucleus-nucleus collisions. Since interaction via one-gluon exchange in QCD contains a spin-orbital coupling, the OAM could cause a global spin polarization of quarks and antiquarks in the direction parallel to the OAM. Such a global (anti)quark polarization should have many observable consequences such as global hyperon polarization [12,13], vector meson spin alignment [12,14], and the emission of circularly polarized photons [15]. Predictions have been made [12,14–17] for these measurable quantities as functions of the global quark polarization P_q. Experimental measurements of the Λ hyperon polarization with respect to the reaction plane at RHIC [18–25] place a limit $|P_{\Lambda,\bar{\Lambda}}| \lesssim 0.02$ [19,24]. Such a limit puts a stringent test on both the initial shear of longitudinal flow in noncentral heavy-ion collisions [17] as well as the time evolution of the polarization through transport processes.

The estimates of the global quark polarization in Ref. [12] and in subsequent studies [16,17,26,27] were all obtained by considering the polarization process for a single scattering between quarks and thermal partons. However, one should consider the effect of the multiple scattering and expect that the quarks will be progressively polarized through multiple scattering. Furthermore, with the minimum values of shear viscosity $\eta/s \geqslant 1/4\pi$ in QGP imposed by the quantum limit, the local momentum shear, dp_z/dx, of the fluid, that is, the local OAM of interacting parton pairs, will decay with time. This will lead to a nontrivial time evolution of quark polarization P depending on the shear viscosity of the QGP matter and the final state observed global polarization could serve as a viscometer of QGP. In this paper, we focus on these two issues with a simple and yet interesting hydrodynamic evolution of a relativistic laminar flow between two frictionless impenetrable walls.

The rest of the paper is organized as follows. In Sec. II, we extend the calculation in Ref. [12] to the case of scattering of an initially polarized quark in a static potential model. In Sec. III, we study the relativistic laminar flow and compute the decay of the longitudinal momentum gradient. The results of Secs. II and III are applied to Sec. IV to study the time evolution of the quark polarization.

II. POLARIZATION OF INITIALLY POLARIZED QUARKS

We consider two colliding nuclei with the beam projectile moving in the direction of $\hat{\mathbf{z}}$ and the impact parameter $\mathbf{b}$ defined as the transverse distance of the projectile from the target nucleus along the $\hat{\mathbf{x}}$ direction as illustrated in the upper panel of Fig. 1. The direction $\hat{\mathbf{y}}$ defines the reaction plane, $\hat{\mathbf{y}} \propto \hat{\mathbf{z}} \times \hat{\mathbf{x}}$. The initial OAM of these two colliding nuclei is along the direction opposite to the reaction plane and could be very large. Given $1\,\text{fm} < b < 10\,\text{fm}$, the initial

OAM $L_0 \simeq Ab\sqrt{s}/2$ is roughly $10^5 \lesssim L_0 \lesssim 10^6$ for Au-Au collisions at RHIC energy $\sqrt{s} = 200$ GeV and $3 \times 10^6 \lesssim L_0 \lesssim 3 \times 10^7$ for Pb-Pb collision at Large Hadron Collider energy $\sqrt{s} = 5.5$ TeV. Because of the unequal local number density of the participant projectile and target nucleons at various transverse positions, some fraction of this large OAM could be transferred into the produced QGP matter in the overlapping region. Such global angular momentum, however, would never lead to a collective rotation of the system since there is no strong binding or attractive interaction in the partonic interaction at high energy. Instead, it could be manifested in the finite transverse (along $\hat{\mathbf{x}}$) gradient of the average longitudinal momentum p_z per produced parton due to the partonic interaction at high energy (see the lower panel of Fig. 1). Given the range of interaction Δx, two colliding partons will have relative longitudinal momentum $\Delta p_z = \Delta x dp_z/dx$ with relative OAM $L_y \sim -\Delta x \Delta p_z$. This relative OAM will lead to global quark polarization along $-\hat{\mathbf{y}}$ through the spin-orbital coupling in QCD. This is essentially the argument that was first proposed in Ref. [12]. It was found that the quark polarization via a single scattering with given relative momentum p reads

$$P \equiv \frac{\Delta\sigma}{\sigma} \equiv \frac{\sigma_\uparrow - \sigma_\downarrow}{\sigma_\uparrow + \sigma_\downarrow} = -\frac{\pi\mu p}{2E(E+m)}, \tag{2.1}$$

where $\sigma_s, s = \uparrow, \downarrow$ is the cross section of final quark with spin s along $\hat{\mathbf{y}}$, m is the mass of interacting quark, and μ is the Debye screening mass of longitudinal gluon, $\mu^2 = g^2(N_c + N_f/2)T^2/3$. The initial relative momentum p can be estimated as $p \simeq \Delta x dp_z/dx$ with $\Delta x \sim \mu^{-1}$ being the characteristic range of interaction. Then p/μ is nothing but the relative orbital angular momentum between the scattering quarks, $L_y \sim -p/\mu$. In the nonrelativistic limit for massive quarks, P is proportional to the spin-orbital coupling energy $P \propto E_{LS}/\mu$, where $E_{LS} = (\vec{L}\cdot\vec{S})(dV_0/dr)/rm^2$ and $(dV_0/dr)/r \sim \mu^3$ with typical interaction range $r \sim 1/\mu$.

The estimates in Refs. [12,16] and [17] were based on the assumption that the initial quarks are not polarized. In order to discuss the time evolution of the quark polarization via multiple scattering, one must calculate the quark-quark cross section of initially polarized quarks. Let the fraction of initial quarks of spin $\lambda_i/2$ along $\hat{\mathbf{y}}$ be $R_{\lambda_i} = (1 + \lambda_i P_i)/2$ with P_i being the initial polarization. The identity $R_+ + R_- = 1$ must hold. Consider a quark with initial relative four-momentum $p^\mu = (E, \mathbf{p})$ and spin $\lambda_i/2$ scattering with a virtual gluon and resulting in final spin $\lambda_f/2$; the cross section with fixed impact parameter $\mathbf{x}_T$ is

$$\begin{aligned}
\frac{d\sigma_{\lambda_f}}{d^2\mathbf{x}_T} &= C_T \sum_{\lambda_i} \int \frac{d^2\mathbf{q}_T}{(2\pi)^2} \int \frac{d^2\mathbf{k}_T}{(2\pi)^2} e^{i(\mathbf{k}_T - \mathbf{q}_T)\cdot\mathbf{x}_T} \\
&\quad \times R_{\lambda_i} \mathcal{I}_{\lambda_f\lambda_i}(\mathbf{k}_T, \mathbf{q}_T, E), \\
\mathcal{I}_{\lambda_f\lambda_i} &\equiv \mathcal{M}_{\lambda_f\lambda_i}(\mathbf{q}_T, E)\mathcal{M}^*_{\lambda_f\lambda_i}(\mathbf{k}_T, E), \\
\mathcal{M}_{\lambda_f\lambda_i}(\mathbf{q}_T, E) &= \frac{g}{2E}\bar{u}_{\lambda_f}(p_q)\not{A}(\mathbf{q}_T)u_{\lambda_i}(p),
\end{aligned} \tag{2.2}$$

where $C_T = 2/9$ is the color factor associated with the target, $\mathbf{q}_T$ ($\mathbf{k}_T$) is the transverse momentum transfer from the virtual gluon to quark, and $p^\mu_{q(k)}$ is the final four-momentum of quark, $p^\mu_{q(k)} = p^\mu + [0, \mathbf{q}_T(\mathbf{k}_T)]$. We use the screened static potential model to calculate $\mathcal{M}_{\lambda_f\lambda_i}$ in which $A^\mu = (A^0, \mathbf{0})$ with $A^0(q_T) = g/(q_T^2 + \mu^2)$ [3].

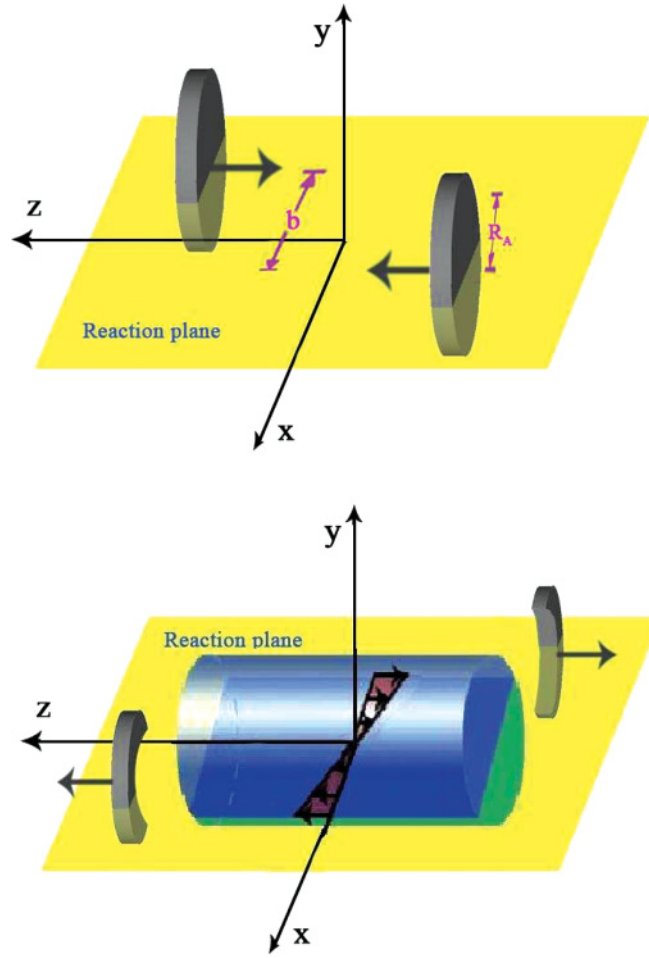

FIG. 1. (Color online) Illustration of noncentral collisions with impact parameter $\mathbf{b}$ of two heavy nuclei with radii R_A. The global angular momentum of the produced matter is along $-\hat{\mathbf{y}}$, opposite to the reaction plane.

For small angle scattering (which is justified when the relative longitudinal momentum $\mathbf{p}$ is large), $q_T, k_T \sim \mu \ll E$, one finds

$$\begin{aligned}
\mathcal{I}_{\lambda_f\lambda_i} \approx \frac{g^2}{2} A_0(q_T)A_0(k_T)\Big\{1 + \lambda_i\lambda_f \\
+ \frac{1}{2E(E+m)}[(1 + \lambda_i\lambda_f)\mathbf{p}\cdot(\mathbf{q}_T + \mathbf{k}_T) \\
+ i(\lambda_i + \lambda_f)\mathbf{p}\cdot\hat{\mathbf{y}}\times(\mathbf{k}_T - \mathbf{q}_T)]\Big\}.
\end{aligned} \tag{2.3}$$

From Eqs. (2.2) and (2.3), it is evident that the polarization will not change if one averages the cross section over all the possible directions of the parton impact parameter $\mathbf{x}_T$. However, in noncentral heavy-ion collisions, the local relative OAM L_y provides a preferred average reaction plane for parton collisions. This will lead to a global quark polarization opposite to the reaction plane of nucleus-nucleus collisions. This conclusion should not depend on our perturbative treatment of

parton scattering as far as the effective interaction is mediated by the vector coupling in QCD. Therefore, we average over the upper half-xy-plane with $x > 0$, that is, average over the relative angle between parton $\mathbf{x}_T$ and the nuclear impact parameter $\mathbf{b}$ from $-\pi/2$ to $\pi/2$ and over x_T. To do this, we use the identity

$$\int_{x>0} d^2\mathbf{x}_T e^{i(\mathbf{k}_T-\mathbf{q}_T)\cdot\mathbf{x}_T} = \frac{2\pi i\delta(k_y-q_y)}{k_x-q_x+i0^+}. \tag{2.4}$$

Then the total unpolarized cross section reads

$$\begin{aligned}\sigma &\equiv \int_{x>0} d^2\mathbf{x}_T \frac{d\sigma}{d^2\mathbf{x}_T} \equiv \int_{x>0} d^2\mathbf{x}_T \left(\frac{d\sigma_+}{d^2\mathbf{x}_T}+\frac{d\sigma_-}{d^2\mathbf{x}_T}\right)\\ &= \int_0^\infty dq_T q_T \frac{C_T g^4}{4\pi\left(q_T^2+\mu^2\right)^2}\\ &\quad\times\left[1-P_i\frac{p\sqrt{q_T^2+\mu^2}K\left(q_T/\sqrt{q_T^2+\mu^2}\right)}{\pi E(E+m)}\right]\\ &= \frac{C_T g^4}{8\pi\mu^2}\left[1-P_i\frac{\pi\mu p}{2E(E+m)}\right],\end{aligned} \tag{2.5}$$

and the polarized cross section reads

$$\begin{aligned}\Delta\sigma &\equiv \int_{x>0} d^2\mathbf{x}_T \frac{d\Delta\sigma}{d^2\mathbf{x}_T} \equiv \int_{x>0} d^2\mathbf{x}_T \left(\frac{d\sigma_+}{d^2\mathbf{x}_T}-\frac{d\sigma_-}{d^2\mathbf{x}_T}\right)\\ &= \int_0^\infty dq_T q_T \frac{C_T g^4}{4\pi\left(q_T^2+\mu^2\right)^2}\\ &\quad\times\left[P_i-\frac{p\sqrt{q_T^2+\mu^2}K\left(q_T/\sqrt{q_T^2+\mu^2}\right)}{\pi E(E+m)}\right]\\ &= \frac{C_T g^4}{8\pi\mu^2}\left[P_i-\frac{\pi\mu p}{2E(E+m)}\right],\end{aligned} \tag{2.6}$$

where $K(x)$ is the complete elliptic integral of the first kind. The final global quark polarization is then

$$P_f = P_i - \frac{\left(1-P_i^2\right)\pi\mu p}{2E(E+m)-P_i\pi\mu p}. \tag{2.7}$$

It is also useful to get the transverse momentum dependence of the quark polarization. From Eqs. (2.5) and (2.6), we read out the differential cross sections,

$$\begin{aligned}\frac{d\Delta\sigma}{dq_T} &= q_T\frac{C_T g^4}{4\pi\left(q_T^2+\mu^2\right)^2}\\ &\quad\times\left[P_i-\frac{p\sqrt{q_T^2+\mu^2}K\left(q_T/\sqrt{q_T^2+\mu^2}\right)}{\pi E(E+m)}\right],\end{aligned} \tag{2.8}$$

$$\begin{aligned}\frac{d\sigma}{dq_T} &= q_T\frac{C_T g^4}{4\pi\left(q_T^2+\mu^2\right)^2}\\ &\quad\times\left[1-\frac{P_i p\sqrt{q_T^2+\mu^2}K\left(q_T/\sqrt{q_T^2+\mu^2}\right)}{\pi E(E+m)}\right].\end{aligned} \tag{2.9}$$

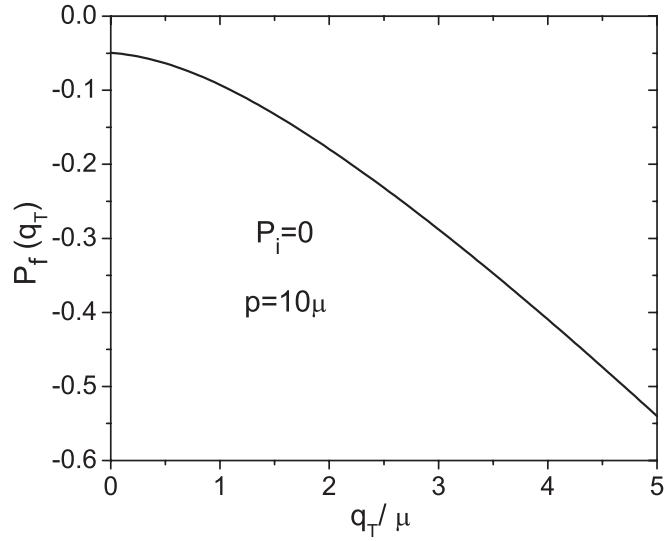

FIG. 2. The TMDP as a function of transverse momentum in unit of μ. The initial relative longitudinal momentum is chosen to be $p = 10\mu$.

The transverse-momentum-dependent polarization (TMDP) defined as $P_f(q_T) \equiv (d\Delta\sigma/dq_T)/(d\sigma/dq_T)$ now reads

$$P_f(q_T) = \frac{\pi E(E+m)P_i - p\sqrt{q_T^2+\mu^2}K\left(q_T/\sqrt{q_T^2+\mu^2}\right)}{\pi E(E+m) - P_i p\sqrt{q_T^2+\mu^2}K\left(q_T/\sqrt{q_T^2+\mu^2}\right)}. \tag{2.10}$$

Some discussions are in order. (i) If the initial quark is unpolarized, $P_i = 0$, we recover the result of Ref. [12]. (ii) Because the denominator is always positive in the right-hand side (RHS) of Eq. (2.7) for high relative longitudinal momentum (i.e., when small angle approximation is applicable), we always have $P_f \leqslant P_i$. Therefore, scattered quarks always prefer to be polarized along $-\hat{\mathbf{y}}$ direction. (iii) The scattering matrix elements $\mathcal{I}_{\lambda_f\lambda_i}$ with spin flipping ($\lambda_f = -\lambda_i$) are zero according to Eq. (2.3), so there is no flipping of quark's spin via the scattering under this small angle approximation. The polarization in the final state is caused by the larger cross section of quarks with spin up relative to quarks with spin down. This will lead to the conclusion that if the initial quark is completely polarized, $P_i = \pm 1$, we must have $P_f = P_i$. This is indeed the case expressed in Eq. (2.7) when $P_i = \pm 1$. (iv) The quark polarization has a remarkable transverse momentum dependence, as shown in Eq. (2.10). Figure 2 shows the typical behavior of TMDP as a function of the transverse momentum with given $p = 10\mu$. The polarization grows with the transverse momentum due to quark-quark scattering. In principle, the Λ-hyperon polarization should have similar transverse momentum dependence, although as we mentioned in Sec. I it is not trivial to construct a correspondence between quark polarization and hadron polarization.

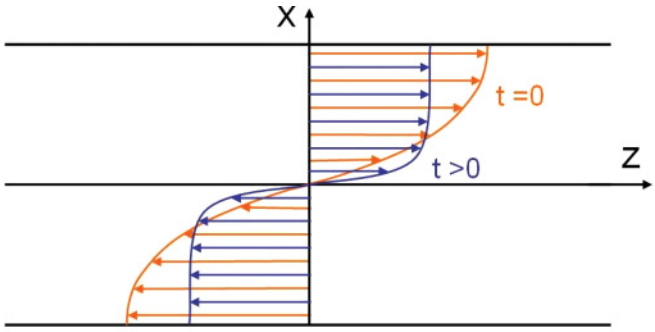

FIG. 3. (Color online) Illustration of the velocity profiles of the relativistic laminar flow.

III. RELATIVISTIC LAMINAR FLOW

Before discussing how the quark polarization evolves in a viscous QGP due to multiple scattering, we have to know how the QGP itself evolves through either transport model or viscous hydrodynamical model [9,10,28–32], Moreover, we also have to know the initial profile of the longitudinal flow field. In the discussion in Sec. II, we simply followed Ref. [12] and assumed that nothing depends on the longitudinal position in the system. In such a case, the finite angular momentum must lead to a velocity profile depicted in Fig. 3 (see Ref. [33] for a discussion of possible consequences of such a profile). On the other hand, another extreme is to assume that $dv_z/dx \equiv 0$ everywhere, but the angular momentum is carried by the matter distribution in the reaction plane; see Ref. [34] for illustration.

To study the effect of viscosity on the decay of the local angular momentum, we consider a simple laminar flow without driving force between two frictionless (free-slip flow) impenetrable walls. We assume the walls are infinitely large and separated by a distance $2h$. To make dimensions relevant for a heavy-ion collision, we set $h = 5$ fm. Such a scenario might be far from the real longitudinal flow profile in high-energy heavy-ion collisions, but it will be very illustrative for our study here. We further assume that the flow profile has no longitudinal variation and the system has a reflection symmetry respect to the yz plane. We study two cases: One with no expansion, and another with boost-invariant expansion in y direction, that is, with flow profile $v_y = y/t$. In both cases, the flow four-velocity in the reaction plane has the general form $u^\mu = (\gamma, \gamma v_x, 0, \gamma v_z)$ with $\gamma \equiv 1/\sqrt{1 - v_x^2 - v_z^2}$ and $v_{x,z}(t, x)$ being the x and z components of the three-velocity.

As is well known, the relativistic Navier-Stokes hydrodynamics is unstable and provides a possibility for acausal signal velocities [35]. Therefore, we use the second-order theory by Israel and Stewart [36] instead. Although hydrodynamics has been widely used to model the heavy-ion collisions, as far as we know, there is no literature discussing the relativistic laminar flow.

If there are no conserved charges, the hydrodynamical equations of motion are given by the conservation of energy and momentum

$$\partial_\mu T^{\mu\nu} = 0, \tag{3.1}$$

where $T^{\mu\nu} \equiv (\varepsilon + \Theta)u^\mu u^\nu - \Theta g^{\mu\nu} + \pi^{\mu\nu}$ is the energy-momentum tensor, ε is the energy density, Θ is the pressure,[1] and $\pi^{\mu\nu}$ is the shear stress tensor. To close the set of differential equations, one also needs to specify an equation of state (EOS) $\varepsilon = \varepsilon(\Theta)$. For simplicity, we use the ideal gas EOS $\varepsilon = 3\Theta$.

In its simplest form, Israel-Stewart hydrodynamics means that instead of being directly proportional to the velocity gradients, the shear stress tensor is a dynamical variable, which relaxes toward the Navier-Stokes value on its relaxation time τ_π:

$$D\pi^{\mu\nu} = -\frac{1}{\tau_\pi}(\pi^{\mu\nu} - 2\eta\nabla^{\langle\mu}u^{\nu\rangle}) - 2\pi^{\kappa(\mu}u^{\nu)}Du_\kappa, \tag{3.2}$$

where $D \equiv u^\lambda\partial_\lambda$, $A^{(\mu\nu)} \equiv (A^{\mu\nu} + A^{\nu\mu})/2$, $A^{\langle\mu\nu\rangle} \equiv [\Delta_\alpha^{(\mu}\Delta_\beta^{\nu)} - \frac{1}{3}\Delta^{\mu\nu}\Delta_{\alpha\beta}]A^{\alpha\beta}$, $\nabla^\mu \equiv \partial^\mu - u^\mu u^\nu\partial_\nu$, $\Delta^{\mu\nu} \equiv g^{\mu\nu} - u^\mu u^\nu$, and η is the shear viscosity coefficient. The last term is required to keep the shear stress tensor orthogonal to the flow velocity in all circumstances. This is the so-called truncated Israel-Stewart equation. Although there are more terms in a complete Israel-Stewart equation, for our purpose here, the truncated one is sufficient.

The relaxation time is given by [36]

$$\tau_\pi = 2\eta\beta_2, \tag{3.3}$$

which is dependent on the shear viscosity and another coefficient β_2. For massless Boltzmann particles, the kinetic theory gives [36]

$$\beta_2 = \frac{3}{4\Theta}. \tag{3.4}$$

If there is no phase transition, it is expected that β_2 for Fermion and Boson gases have only minor modification from β_2 for Boltzmann gas at high temperature [37–42]. Taking temperature $T \sim 350$ MeV, the relaxation time is around $\tau_\pi \sim 0.27$–1.35 fm if using $\eta/s = 1/(4\pi) - 5/(4\pi)$, where s is the entropy density, and for free gluon gas it is

$$s = \nu_g\frac{2\pi^2T^3}{45}, \tag{3.5}$$

with the degeneracy factor $\nu_g = 2(N_c^2 - 1)$.

Since the system has reflection symmetry with respect to the yz plane, and there are no particle, momentum, or heat flow through the hard walls, the system obeys the following boundary conditions:

$$\begin{aligned} v_z(t, 0) = v_x(t, 0) = v_x(t, \pm h) = 0, \\ \partial v_z(t, \pm h)/\partial x = 0. \end{aligned} \tag{3.6}$$

As the initial state we choose uniform initial temperature of 355 MeV (corresponding to RHIC initial temperature), no flow in x direction, and a simple sine-type longitudinal flow velocity profile

$$\begin{aligned} v_x(t_0, x) = 0, \\ v_z(t_0, x) = v_0\sin(\pi x/2h), \end{aligned} \tag{3.7}$$

[1]Note that since we used P to denote polarization, to avoid confusion we do not use it to denote pressure.

where v_0 is the magnitude of the initial velocity at the two boundaries. In the following numerical calculation, we consider two cases: $v_0 = 0.7$ and 0.9. In the expanding case, we use the initial time $\tau_0 = 1$ fm. Since the shear stress tensor is a dynamical variable in Israel-Stewart hydrodynamics, we need its initial value too. A natural choice is the Navier-Stokes value, but its exact evaluation is difficult. It contains the time derivative of the flow velocity, which is unknown before the hydrodynamic equation is solved. To avoid this problem, we initialize the shear stress, not to its exact Navier-Stokes, but to a "static Navier-Stokes" value; that is, we ignore all the time derivatives in the Navier-Stokes definition of the shear stress tensor and calculate the value based on spatial derivatives only. In practice this means that some components of the tensor are slightly larger and some slightly smaller than their exact Navier-Stokes values.

In Fig. 4, we depict the time evolution of the gradient of the longitudinal momentum per particle averaged over $x \in [0, h]$,

$$\left\langle \frac{dp_z}{dx} \right\rangle \equiv \int_0^h dx J^0(x) \frac{d}{dx} \frac{T^{0z}(x)}{J^0(x)} \Big/ \int_0^h dx J^0(x), \qquad (3.8)$$

where $J^0 = \gamma\rho$ is the proper particle number density. As expected, the shear viscosity dissipates the average gradient of the longitudinal momentum, especially for larger values of shear viscosity. The transverse expansion accelerate this degradation, since strong transverse expansion means larger shear (shear tensor).

In the case of transverse expansion and large viscosity, there appear to be a "shoulder" in the time evolution of the longitudinal momentum gradient $\langle dp_z/dx \rangle$ as shown in the lower panel of Fig. 4, where the gradient drops very fast initially and then slows down for a while before it decreases again. The temporary slowdown is caused by the oscillatory behaviors of the induced transverse flow in the x direction, and the particle number density J^0, which is used as a weight in the calculation of the average longitudinal momentum gradient in Eq. (3.8). The oscillations are an artifact of the fixed-wall boundary conditions in our simple scenario. When there is no transverse expansion, the degradation is slower and there is no shoulder because of the smaller shear (in shear tensor).

In Fig. 5, we show the profiles of velocity v_z at different times with viscosity $\eta/s = 5/4\pi$ with (lower panel) and without (upper panel) transverse expansion. One of the functions of the shear viscosity is to transform the kinetic energy of the fluid to internal energy, hence damping the fluid shear (as shown in Fig. 5) and heating up the fluid. This can be explicitly seen in the upper panel of Fig. 6, where the temperature evolution is shown for the nonexpanding system. The transverse Bjorken expansion in our problem, however, will dilute the system and cool the system down, overcoming the slight heating up by the shear viscosity, as shown in the lower panel of Fig. 6. The transverse expansion will also accelerate the degradation of the longitudinal velocity as shown in the lower panel of Fig. 5 as compared to the upper panel for the case of no transverse expansion.

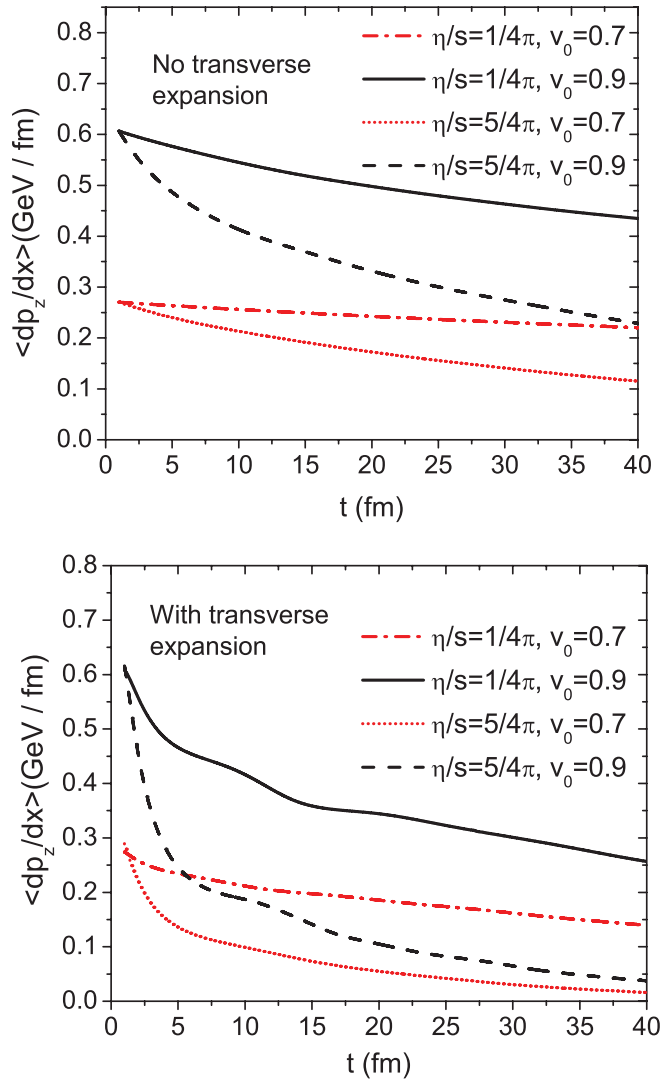

FIG. 4. (Color online) Evolution of the average gradient of the longitudinal momentum per particle, dp_z/dx, at different shear viscosities. Upper panel: the system has no transverse expansion. Lower panel: the system has Bjorken expansion in the $\hat{\mathbf{y}}$ direction.

IV. EVOLUTION OF THE GLOBAL QUARK POLARIZATION

With the model of time evolution of the longitudinal momentum gradient of the medium partons, we can now study the time evolution of the quark polarization when it is progressively polarized due to multiple scattering.

According to Eq. (2.7), the change of polarization caused by one scattering is

$$\Delta P \equiv P_f - P_i = -\frac{(1 - P_i^2)\pi\mu p}{2E(E + m) - P_i \pi \mu p}. \qquad (4.1)$$

For convenience, we denote $P = P_i$. Then we get the following evolution equation for the polarization:

$$\frac{dP}{dt} \equiv \frac{\Delta P}{\tau_q} = -\frac{1}{\tau_q} \frac{(1 - P^2)\pi\mu p}{2E(E + m) - P\pi\mu p}, \qquad (4.2)$$

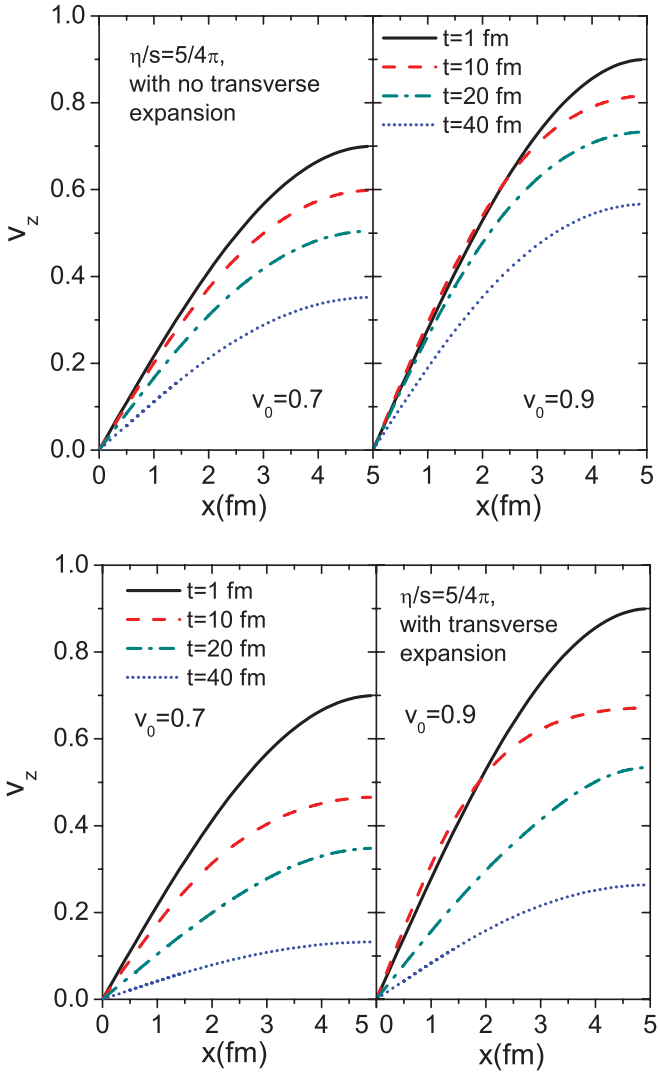

FIG. 5. (Color online) The profile of longitudinal velocity v_z at different times with $\eta/s = 5/4\pi$.

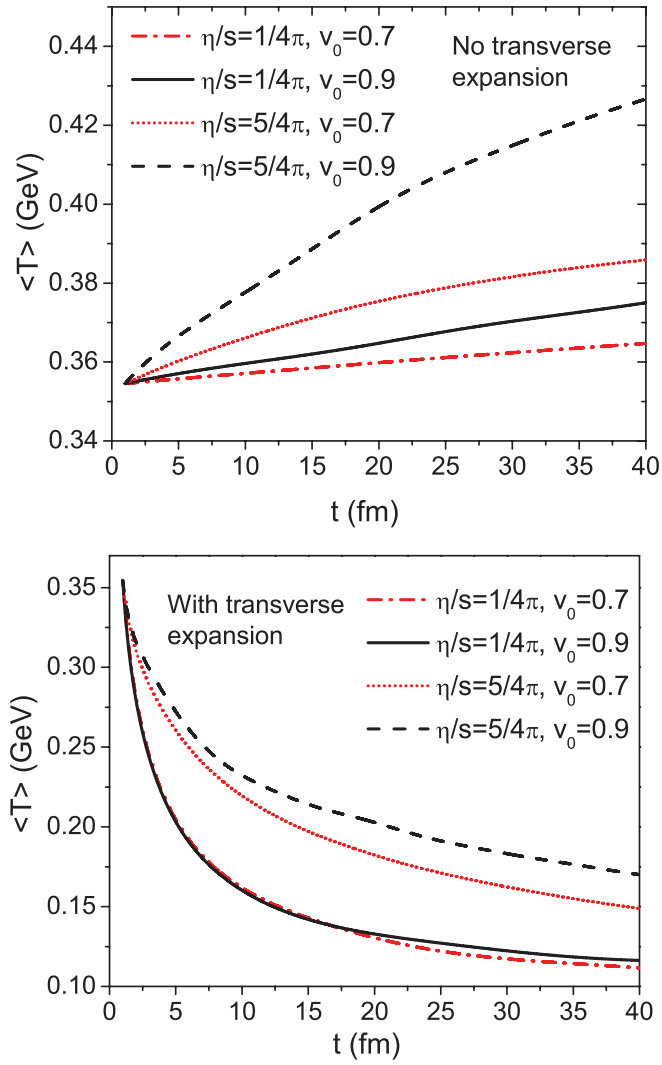

FIG. 6. (Color online) Evolution of the average temperature $\langle T \rangle$ with different shear viscosities and different initial velocities. Upper panel: the system has no transverse expansion. Lower panel: the system is Bjorken expanding in the $\hat{\mathbf{y}}$ direction.

where τ_q is the mean free path of quark, which is related to the transport cross section $\sigma_{\rm tr}$ of the interacting partons though $\tau_q \simeq 1/(\rho\sigma_{\rm tr})$, where $\rho = \nu_g \zeta(3) T^3/\pi^2$ is the density of medium gluons, assuming gluons are the dominant degrees of freedom in the medium. The shear viscosity for a thermal ensemble of gluons is roughly [43]

$$\eta \simeq \tfrac{1}{3}\rho\langle p_{\rm tr}\rangle \tfrac{4}{9}\tau_q \approx T\tfrac{4}{9}\rho\tau_q. \tag{4.3}$$

We have then the final rate equation for the time evolution of the quark polarization,

$$\frac{dP}{dt} = -\frac{4T\rho}{9s}\frac{s}{\eta}\frac{(1-P^2)\pi\mu p}{2E(E+m)-P\pi\mu p}. \tag{4.4}$$

From Eq. (4.4), the rate dP/dt is inversely proportional to the viscosity. This is evidently shown in the upper panel of Fig. 7, in which the evolutions of the quark polarizations are shown for the initial polarizations $P(0) = 0$ and for a system without transverse expansion. With transverse expansion, the mean free path increases more rapidly with time and therefore slows down the polarization rate. The transverse expansion also accelerates the degradation of the longitudinal momentum gradient, reducing the polarization in each scattering. Both effects slow down the time evolution of the polarization in an expanding system as shown by comparison between the upper and lower panels of Fig. 7.

Because of the reheating by viscous interaction, the initial cooling of the system due to transverse expansion is significantly slower for a larger value of shear viscosity, as shown in Fig. 6. This speeds up the polarization according to Eq. (4.4). However, a larger shear viscosity also slows down the polarization because the polarization rate is inversely proportional to the shear viscosity. During the early stage of evolution, the second effect dominates, leading to a slower polarization process with a larger value of shear viscosity. At a later time, effect of reheating becomes more dominant and a larger shear viscosity leads to a faster polarization process.

The polarization is also sensitive to the initial condition of the longitudinal flow shear. In our simple laminar flow model, the initial longitudinal flow shear is proportional to the value

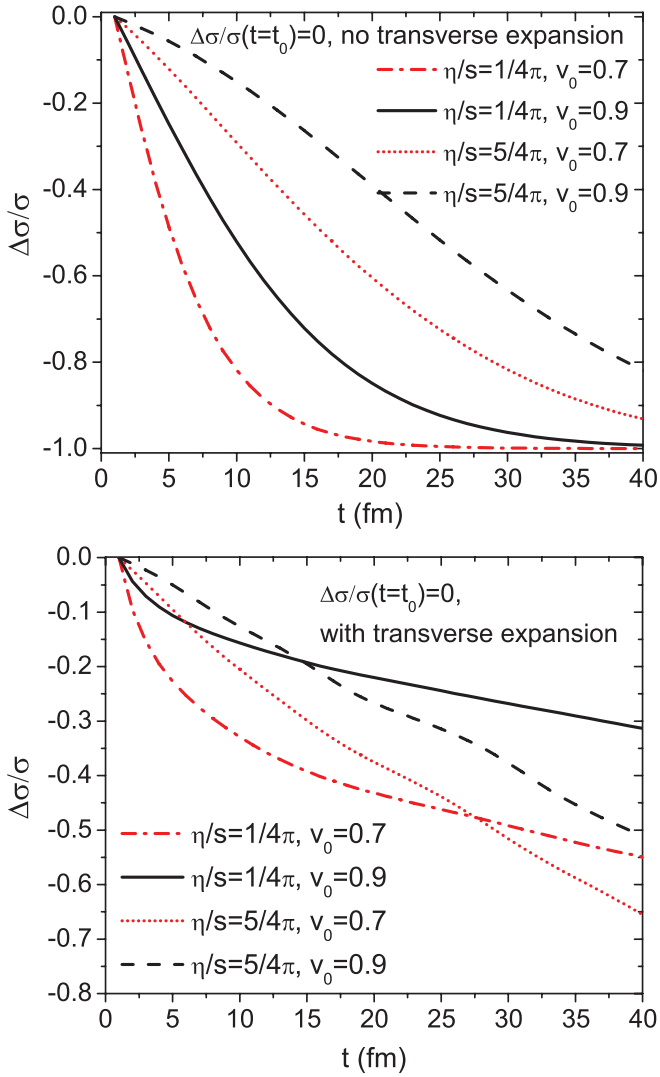

FIG. 7. (Color online) Evolution of the average polarization $P = \Delta\sigma/\sigma$ with initial polarization $P(t_0) = 0$ with different values of viscosities without (upper panel) and with (lower panel) transverse expansion.

of v_0. The nonlinear dependence of the polarization rate on the relative momentum p in Eq. (4.4) determines the nontrivial dependence of the polarization on the values of v_0 as shown in Fig. 7.

Note that the polarization rate we used are derived with the approximation of small angle scattering, which is only valid when the longitudinal momentum gradient is large. For large shear viscosity η/s and at late time, the longitudinal momentum gradient can become too small. One can no longer use the rate equation derived here. However, one can assume that the polarization process will stop at this point when there is not significant local orbital angular momentum.

V. SUMMARY

In conclusion, we have calculated the polarization cross section for quarks with initial polarization within the frame of perturbative QCD, which we use to study the time evolution of the quark polarization via multiple scattering in a medium with nonvanishing local orbital angular momentum. We considered the simple case of laminar flow as governed by viscous hydrodynamics with given shear viscosity η/s and a simple illustrative initial condition. Such a simple hydrodynamic model provides the dynamic evolution of the longitudinal flow shear as the polarization mechanism for quarks via parton scattering. Because the values of the shear viscosity influence the degradation of the longitudinal flow shear with time and the cooling of the system, it also determines the time evolution of the quark polarization. Since the polarization rate is inversely proportional to the shear viscosity and depends nonlinearly on the average longitudinal momentum shear, the final quark polarization is found to be sensitive to the shear viscosity but has a nontrivial dependence. In this sense, one can use the final-state polarization as a possible viscometer of the QGP.

For more realistic studies, one should employ a full scale $3 + 1D$ viscous hydrodynamics [32] with initial conditions from Monte Carlo models such as HIJING [44]. The initial parton production from this kind of model has approximate Bjorken scaling, which will give rise to very small initial local longitudinal flow shear [17] except at very large rapidity regions. Such small initial local longitudinal flow shear comes from the violation of the Bjorken scaling, which one can use as the initial condition. Furthermore, one should also extend the current calculation of the quark polarization beyond the small angle approximation.

ACKNOWLEDGMENTS

We thank G. Torrieri, D. Rischke, and Z. Xu for helpful discussions. This work is supported by the Helmholtz International Center for FAIR within the framework of the LOEWE (Landesoffensive zur Entwicklung Wissenschaftlich-Ökonomischer Exzellenz) program launched by the State of Hesse, by the ExtreMe Matter Institute (EMMI), and by BMBF under Contract No. 06FY9092 and by the director, Office of Energy Research, Office of High Energy and Nuclear Physics, Divisions of Nuclear Physics, of the US Department of Energy under Contract No. DE-AC02-05CH11231. X.-N. Wang thanks the hospitality of the Institut für Theoretische Physik, Johann Wolfgang Goethe-Universität, and support by EMMI in the framework of the Helmholtz Alliance Program of the Helmholtz Association (HA216/EMMI) during the beginning of this work.

[1] M. Gyulassy and L. McLerran, Nucl. Phys. A **750**, 30 (2005).
[2] P. Jacobs and X. N. Wang, Prog. Part. Nucl. Phys. **54**, 443 (2005).
[3] M. Gyulassy and X. N. Wang, Nucl. Phys. B **420**, 583 (1994).
[4] B. G. Zakharov, JETP Lett. **63**, 952 (1996).
[5] U. A. Wiedemann, Nucl. Phys. B **588**, 303 (2000).

[6] M. Gyulassy, P. Levai, and I. Vitev, Nucl. Phys. B **594**, 371 (2001).
[7] R. Baier, Y. L. Dokshitzer, A. H. Mueller, S. Peigne, and D. Schiff, Nucl. Phys. B **483**, 291 (1997).
[8] X. F. Guo and X. N. Wang, Phys. Rev. Lett. **85**, 3591 (2000).
[9] M. Luzum and P. Romatschke, Phys. Rev. C **78**, 034915 (2008); **79**, 039903(E) (2009).
[10] H. Song, S. A. Bass, U. Heinz, T. Hirano, and C. Shen, Phys. Rev. Lett. **106**, 192301 (2011).
[11] A. Majumder, B. Muller, and X. N. Wang, Phys. Rev. Lett. **99**, 192301 (2007).
[12] Z. T. Liang and X. N. Wang, Phys. Rev. Lett. **94**, 102301 (2005); **96**, 039901 (2006).
[13] B. Betz, M. Gyulassy, and G. Torrieri, Phys. Rev. C **76**, 044901 (2007).
[14] Z. T. Liang and X. N. Wang, Phys. Lett. B **629**, 20 (2005).
[15] A. Ipp, A. Di Piazza, J. Evers, and C. H. Keitel, Phys. Lett. B **666**, 315 (2008).
[16] Z. T. Liang, J. Phys. G **34**, S323 (2007).
[17] J. H. Gao, S. W. Chen, W. T. Deng, Z. T. Liang, Q. Wang, and X. N. Wang, Phys. Rev. C **77**, 044902 (2008).
[18] STAR Collaboration, I. V. Selyuzhenkov *et al*., Rom. Rep. Phys. **58**, 49 (2006).
[19] STAR Collaboration, I. Selyuzhenkov *et al*., J. Phys. G **32**, S557 (2006).
[20] STAR Collaboration, I. Selyuzhenkov *et al*., AIP Conf. Proc. **870**, 712 (2006).
[21] STAR Collaboration, I. Selyuzhenkov *et al*., J. Phys. G **34**, S1099 (2007).
[22] STAR Collaboration, B. I. Abelev *et al*., Phys. Rev. C **76**, 024915 (2007).
[23] STAR Collaboration, B. I. Abelev *et al*., Phys. Rev. C **77**, 061902 (2008).
[24] STAR Collaborations, J. H. Chen *et al*., J. Phys. G **34**, S331 (2007).
[25] STAR Collaboration, J. H. Chen *et al*., J. Phys. G **35**, 044068 (2008).
[26] S. W. Chen, J. Deng, J. H. Gao, and Q. Wang, Front. Phys. China **4**, 509 (2009).
[27] J. H. Gao, High Energy Phys. Nucl. Phys. **31**, 1181 (2007).
[28] K. Dusling and D. Teaney, Phys. Rev. C **77**, 034905 (2008).
[29] H. Song and U. W. Heinz, Phys. Lett. B **658**, 279 (2008).
[30] D. Molnar and P. Huovinen, J. Phys. G **35**, 104125 (2008).
[31] G. S. Denicol, T. Kodama, T. Koide, and Ph. Mota, Phys. Rev. C **80**, 064901 (2009).
[32] B. Schenke, S. Jeon, and C. Gale, Phys. Rev. Lett. **106**, 042301 (2011).
[33] F. Becattini, F. Piccinini, and J. Rizzo, Phys. Rev. C **77**, 024906 (2008).
[34] A. Adil and M. Gyulassy, Phys. Rev. C **72**, 034907 (2005).
[35] W. A. Hiscock and L. Lindblom, Ann. Phys. **151**, 466 (1983).
[36] W. Israel and J. M. Stewart, Ann. Phys. **118**, 341 (1979).
[37] R. Baier, P. Romatschke, D. T. Son, A. O. Starinets, and M. A. Stephanov, J. High Energy Phys. **0804**, 100 (2008).
[38] M. Natsuume and T. Okamura, Phys. Rev. D **77**, 066014 (2008); **78**, 089902(E) (2008).
[39] M. A. York and G. D. Moore, Phys. Rev. D **79**, 054011 (2009).
[40] B. Betz, D. Henkel, and D. H. Rischke, Prog. Part. Nucl. Phys. **62**, 556 (2009); G. S. Denicol, T. Koide, and D. H. Rischke, Phys. Rev. Lett. **105**, 162501 (2010).
[41] T. Koide, E. Nakano, and T. Kodama, Phys. Rev. Lett. **103**, 052301 (2009).
[42] G. S. Denicol, X. G. Huang, T. Koide, and D. H. Rischke, arXiv:1003.0780 [hep-th]; X. G. Huang and T. Koide, arXiv:1105.2483 [hep-th].
[43] P. Danielewicz and M. Gyulassy, Phys. Rev. D **31**, 53 (1985).
[44] X. N. Wang and M. Gyulassy, Phys. Rev. D **44**, 3501 (1991).